A Simple, Membrane-Free, Direct Glycerol Fuel Cell Utilizing a Precious Metal-Free Cathode and Gold-Plated Anode Surfaces

Yi Jie Tseng and Daniel Scott *

Natural Sciences Department, Brigham Young University–Hawaii, Laie, HI 96762-1294, USA;
yijietseng@gmail.com
* Correspondence: daniel.scott@byuh.edu; Tel.: +1-808-778-6831

Abstract: As bio-diesel production continues around the world, the amount of low-grade glycerol, a byproduct from the process, in increasing, as is the demand for a simple, easy-to-make, fuel cell capable of running off glycerol and oxygen from the air. Despite the research that has already been done with glycerol fuel cells, the complexity of the fuel cell designs for such a simple fuel appears to be prohibitive toward the actualization of such a cell. Here the simplest of fuel cells, an alkaline, membrane-free, glycerol fuel cell with a non-platinum-containing MnO_2 cathode is explored. Glycerol oxidation is catalyzed on various surfaces including carbon felt, platinum, and silver-plated nickel with and without gold plating. The maximum power this glycerol fuel cell generates, with 1.4 M glycerol and 8.0 M KOH, is 1.27 mW cm^{-2} at 200 mV. It has an open circuit voltage of 704 mV. Additionally, the effects of different, gold-plated anodic surfaces, electrolytes and temperatures are also explored. This work demonstrates the feasibility of this simple, reusable robust cell design using pure and crude glycerol from bio-diesel production and preliminarily explores the products of this reaction.

Keywords: glycerol; direct fuel cell; platinum-free cathode; membrane-less; gold-plated anode

1. Introduction

As the population continues to grow around the world, there is an ever-increasing need for clean and efficient sources of energy. As it is also likely that future energy needs will come from multiple power sources that work in concert, there is an implied need to diversify the sources of produced energy [1,2]. This diversification will also contribute to the ability to remotely power smaller electronic devices under a variety of situations.

Although it is inconceivable to think that hydrocarbons will be replaced as an energy source any time soon, there is always an ever pressing need to improve the efficiency of the use of all traditional energy resources, including small molecule carbon compounds. One high energy small molecule hydrocarbon that has proved resistant to use as a non-biological energy source is glycerol. The visibility of glycerol has increased in parallel with the development of the bio-diesel industry as the latter has continued to grow over the past 20 years [3]. The production of bio-diesel utilizes the base-catalyzed transesterification of waste vegetable oil with methanol to make renewable fuel for transportation or other diesel dependent systems. Additionally, as bio-diesel exploitation increases, the large amount of low-grade glycerol byproduct produced has begun to impact the sustainability of the whole bio-diesel production process.

Bio-diesel production results in a volume of approximately 10% (*w/w*) glycerol of the total product [4]. Although many uses have been touted, the oversupply of crude glycerol byproduct remains

a deterrent to the further promotion of bio-diesel production and its use. Entities investing in bio-diesel production also need to begin to consider investing in glycerol storage. As a result, some research has been done to convert glycerol into smaller carbon-containing molecules for alternative energy applications [5–7]. This conversion work appears to be too energy intensive and will likely not result in a feasible way to use the glycerol feedstock as an energy source anytime soon.

Glycerol is difficult to use as an energy source in a traditional combustive manner and has been only non-biologically approachable through fuel cell designs [8]. Biologically, glycerol has been used a variety of ways, including to grow bacteria or livestock, to conserve energy, or to produce an alternative energy source [9].

Fuel cells are arguably the most efficient way to harvest energy from a resource as the process avoids the limitations of the Carnot cycle and harnesses an increased amount of the available energy. Research has been invested into the development of fuel cell configurations to generate power directly from glycerol oxidation with different anodic materials and catalysts [10–12]. In recent studies, the catalytic oxidation of glycerol was found to be significantly promoted by the presence of gold and platinum catalysts on carbon supports under alkaline conditions [13–17]. These are conditions which are similar to fuel cells that have utilized other alcohols or sugar alcohols such as methanol, ethanol, and ethylene glycol [18].

For the most part, these fuel cell designs are modeled after the hydrogen fuel cell with expensive precious metal catalysts at the cathode and temperamental separator membranes [10,11,14,16–26]. Such cells can require a significantly skilled level of expertise to fabricate them. Of the ten glycerol fuel cells compared in researching these efforts, all but four use a platinum-based catalyst at the cathode. Of the ten, all used some form of a proton exchange membrane. Again, these choices are generally based on modeling these fuel cells after the hydrogen fuel cell. The proton exchange membrane is arguably one of the limiting factors in the commercialization of the hydrogen fuel cell and is really not feasible if a fuel cell for glycerol is going to be further developed. This fact is accentuated by the use of a proton exchange membrane in the example of a bio-fuel cell that uses biological catalysts at the anode and cathode. Even though the catalysts are generally exclusive in terms of their substrate preferences, this cell also uses a proton exchange membrane (Table A1).

In this work, extremely simple glycerol fuel cells were made from a purchased MnO_2 cathode catalyst material. Various materials, with and without gold-coating, were used as anodic surfaces. A non-conductive material (a piece of plastic with holes) was used as a separator to ensure that the anode and the cathode did not come in contact. The cell electrolyte was aqueous KOH. Glycerol was added to the electrolyte, completing the fuel cell.

These simple cells can collect a significant amount of energy from glycerol under basic conditions without a membrane. The performance of these glycerol fuel cells was also recorded at different temperatures. Additionally, experiments using various concentrations of ethanol, xylitol, and glucose were performed to compare with the glycerol fuel cell. To ensure this cell design was able to generate power from crude glycerol, glycerol from a batch of bio-diesel was produced through the transesterification of oil with methanol and KOH, and the crude glycerol was also used as the fuel for this simple fuel cell.

After the performance of the cell was evaluated and the dependence of the cell's performance on the concentration of glycerol and KOH was determined, a preliminary survey into the products of this oxidation was begun. Product determination was explored with nuclear magnetic resonance (NMR), an enzymatic peroxidase assay, a pressure assay to detect the production of gasses from the products, and comparative titrations. All of these methods and assays were to help contribute to the future identification of possible products of this oxidation reaction occurring in the fuel cell.

2. Materials and Methods

2.1. Reagents

Glycerol ($\geq$99.5%) was purchased from Fisher Scientific (Logan, UT, USA). Potassium cyanide (KCN) was purchased from Fluka Analytical (München, Germany) Potassium hydroxide (KOH) pellets were purchased from VWR Analytical (New York City, NY, USA). A 20 mM solution of gold chloride ($AuCl_3$) was purchased from Unit-Tech (St. Louis, MO, USA). Methanol, ethanol, xylitol, glucose, equine heart myoglobin, potassium chloride (KCl), Tris base, sodium malonate, potassium oxalate, and 2,2′-azino-bis (3-ethylbenzothiazoline-6-sulphonic acid) (ABTS), and manganese (IV) oxide (MnO_2) were purchased from Sigma-Aldrich (St. Louis, MO, USA).

2.2. Fuel Cell Materials

Glycerol fuel cells were simply made from the cathodic material utilizing different anodic surfaces. The materials used as anodic surfaces were 99% gold mesh (6.25 cm^2), platinum mesh, gold-plated platinum mesh (5.28 cm^2), carbon felt, gold-plated carbon felt (5 cm^2, 3.18 mm thick), silver-plated nickel mesh, and gold-plated sliver-plated nickel mesh (4.94 cm^2). All connecting wires were made of platinum to nullify any corrosive currents from contributing to the produced power.

For the preparation of the gold-plated surfaces, a solution of 10 mM $AuCl_3$ and 1.6 M KCN was prepared, and a 9V battery was used to provide the plating potential. A platinum wire was used as a counter electrode for gold plating. After connecting all surfaces, the surfaces and the counter electrode were dipped into the solution for 10 s. All gold-plated surfaces were prepared this way. The air-breathing cathode (a silver-plated nickel screen electrode with 0.6 mg cm^{-2} loading using 10% MnO_2 on Vulcan XC-72 with micro-porous fluorocarbon backing) was purchased from Electric Fuel (Bet Shemesh, 9905415, Israel). Cells were organized in-house by simply using a heat gun to seal the micro-porous fluorocarbon backing on both sides of the cathode and an adhesive (white Gorilla Glue, Gorilla Glue Company, Sharonville, OH, USA) to strengthen the seal. The resulting cells have a thin V-shaped structure (Figure 1). The volumes of the cells are approximately 3 mL.
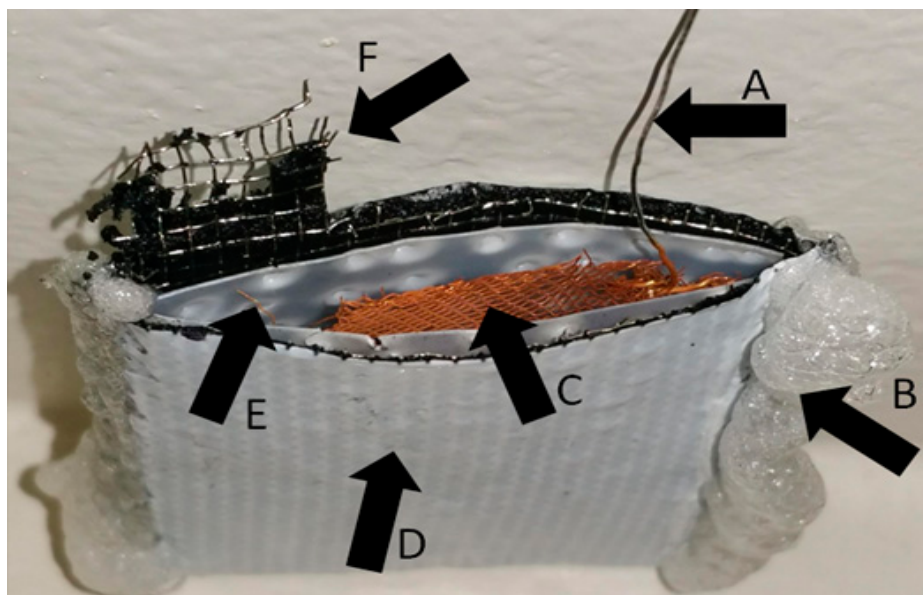

Figure 1. This is the V-shape cell type used in these experiments. (A) Platinum wire used to connect the anode to avoid corrosion contributing to the power output. (B) Adhesive used to prevent leaking. (C) Gold-plated platinum mesh used as the anodic surface. (D) Air-breathing cathode material. (E) Plastic with holes used to prevent electrode contact. (F) Current collecting framework of the air-breathing cathode material.

2.3. Experimental and Methods

Fuel cell experiments were performed with different concentrations of glycerol (0.27 molar (M), 0.68 M, 1.4 M, 4.1 M, 8.2 M) and KOH (0.5 M, 1 M, 3 M, 6 M, 8 M). Additionally, experiments with different concentrations of ethanol (0.34 M, 1.7 M, 10 M), xylitol (0.2 M, 0.5 M, 1 M), and glucose (0.2 M, 0.5 M, 1 M) were performed, also in solutions of 8 M KOH. Power was drawn from glycerol cells in which the above listed anodic surfaces were used. The concentration of glycerol and OH^- in the bio-diesel glycerol byproduct was determined by comparing the completion of the transesterification reaction, the solutions pH and was confirmed by using the resulting voltages upon drawing currents and comparing those voltages to a standard curve created from previous experiments (Figure A1).

The final product of the oxidation of glycerol in these fuel cells was explored with ^{13}C-NMR, a colorimetric ABTS peroxidase assay, a pressure assay, and a set of comparative titration experiments. The peroxidase enzymatic activity of myoglobin was harnessed to identify the presence of H_2O_2 as a byproduct of the oxidation of glycerol by monitoring the changing absorbance of the electron donor ABTS in solution with a spectrophotometer. All measurements were performed in 1M tris buffer pH 7.5 with a total volume of 3 mL. The pH of the fuel sample was adjusted to about 7.5, and 0.02 mL of the sample was added along with 0.1 mL of ABTS and 0.2 mL of a 2 mg mL^{-1} myoglobin solution.

A pressure assay was also performed which can relate an increase in pressure to the release of a gas from solution. This assay can be used to detect the presence of either H_2O_2 or the carbonate ion. These two types of experiments were performed by either adding MnO_2 to detect H_2O_2, or HCl to detect the presence of the carbonate ion. Solutions of (a) 8 M KOH and 100 μL H_2O_2, (b) 8 M KOH and an unreacted sample of 1.4 M glycerol, and (c) a reacted sample which initially contained 8 M KOH and 1.4 M glycerol were compared to each other. To show MnO_2 can decompose H_2O_2 under neutral and basic conditions, two controls were set up. Control 1 was suspension of MnO_2 with 100 μL H_2O_2; control 2 was a suspension of MnO_2 with 100 μL H_2O_2 and 8 M KOH. The pressure changes were monitored through a Micro LAB interface. Additionally, to determine if the gas produced by the reacted solutions was something other than oxygen, an oxygen sensor was used to detect its relative concentration before and after the pressure change in the reaction vessel. The change in pressure can also indicate the amount of gas and thus the amount of either reactant in the initial sample.

A titration was also performed on the reacted fuel cell sample as well. The reacted sample (8 M KOH and 1.4 M glycerol after oxidation) was titrated with 0.1 M HCl. Three compounds were used to attempt to simulate the titration curve of the sample. These compounds were carbonate, malonate and oxalate in a comparable solution of KOH. The titration curve was also monitored by a Micro LAB interface in which the pH was monitored vs. the volume of added HCl.

2.4. Instrumentation

All electrochemical measurements were obtained using a Bio-Logic 3-channel VSP galvanostat/potentiostat (Bio-Logic Science Instruments, Seyssinet-Pariset, France). Electrochemical cells were monitored at different current levels to determine sustainable voltages. The anodic surfaces were coated with a thin gold surface through applying voltage to the anodes' surfaces in the mixture of potassium cyanide, potassium hydroxide, and gold chloride with a platinum wire as the counter electrode. The ABTS assay was monitored by the kinetics application of the Vernier SpectroVis Plus spectrophotometer software (Vernier Software & Technology, Beaverton, OR, USA). Additionally, the pressure assay and titrations were performed on a FS-522 MicroLab system (MicroLab, Moscow, Russia) with qualitative oxygen measurements taken with a DO200 Oxygen sensor from YSI Environmental (Yellow Springs, OH, USA). An UltraShield 300 NMR instrument (Bruker, Billerica, MA, USA) was used to help in the identification of the final products after glycerol oxidation.

3. Results

3.1. Optimization of Glycerol and KOH Concentrations

Table 1 describes the combinations of various concentrations of different fuel sources (glycerol, ethanol, xylitol and glucose) in various concentrations of KOH with different anodic surfaces and their corresponding power outputs. All data in Table 1 were obtained from experiments at 25 °C. The glycerol fuel cell with 8 M KOH and 1.4 M glycerol was able to produce a maximum power output of 1.27 mW cm^{-2}, and the open circuit voltage was 704 mV as shown in Figure 2.

Table 1. Various combinations of electrolyte solutions with different anodic surfaces and their corresponding average power outputs.

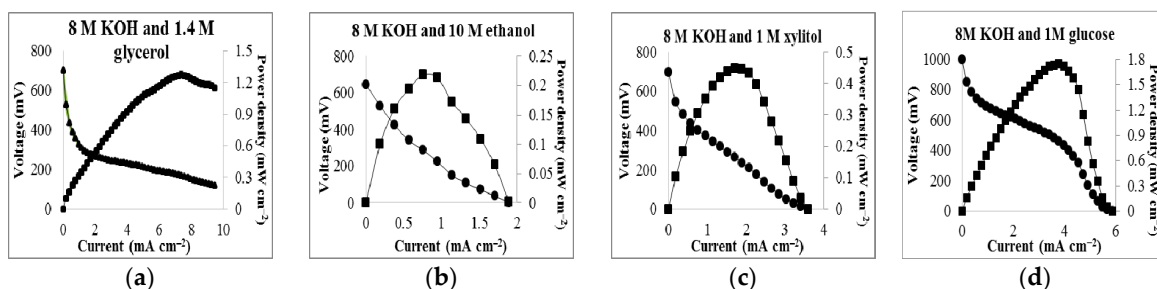| Anode Material	Fuel Source	Concentrations of Fuel Source (M)	Concentrations of KOH (M)	Average Open Circuit Voltage (mV)	Maximum Power (mW cm^{-2})
Au-plated platinum mesh (5.28 cm^2)	Glycerol	0.27 M	8 M	433	0.081
		0.68 M		545	0.223
		1.4 M		704	1.27
		4.1 M		730	0.750
		8.2 M		774	0.601
		1.4 M	0.5 M	315	0.067
			1 M	338	0.117
			3 M	467	0.223
			6 M	581	0.542
			8 M	704	1.27
	Ethanol	0.34 M		569	0.030
		1.7 M		704	0.050
		10 M		647	0.218
	Xylitol	0.2 M		546	0.126
		0.5 M		615	0.236
		1 M		694	0.447
	Glucose	0.2 M		866	0.597
		0.5 M		939	1.27
		1 M		1000	1.74
	Crude Glycerol	1.26 M		613	0.410
Pt mesh (6.25 cm^2)	Glycerol	1.4 M	8 M	645	0.199
Carbon felt (5 cm^2)				130	0
Au-plated Carbon felt (5 cm^2)				519	0.134
Ag-Ni mesh (4.94 cm^2)				229	0
Au-plated-Ag-Ni mesh (4.94 cm^2)				394	0.132
99% Gold mesh				492	0.057

Figure 2. Polarization curve and power output for (**a**) 1.4 M glycerol in 8 M KOH solution; (**b**) 10 M ethanol in 8 M KOH solution; (**c**) 1 M xylitol in 8 M KOH solution; (**d**) 1 M glucose in 8 M KOH solution.

Figure 2 also displays the maximum performances for ethanol, xylitol, and glucose. Figure 3 demonstrates the cell's voltage dependence on varying concentrations of glycerol and KOH. Experiments were performed in which glycerol concentrations of 0.27 M, 0.68 M, 1.4 M, 4.1 M, and 8.2 M in 8 M KOH were used as the cell's fuel/electrolyte. To show power dependence on KOH, experiments were performed in which concentrations of KOH of 0.5 M, 1 M, 3 M, 6 M, and 8 M, were used in the presence of 1.4 M glycerol. Although power production increased as glycerol concentrations increased, there was an unexpected decrease in power production when the concentration of glycerol increased to 4.1 M. Optimal power production was observed under conditions of 8 M KOH and 1.4 M glycerol with a power of 1.27 mW cm^{-2} at 7.39 mA/cm^2 solution (see Figure 3a).The reaction is also dependent on the concentration of KOH as depicted in Figure 3b. As the concentration of KOH increased, the power output also increased. To further investigate the effect from KOH, the combination of the electrolyte was changed. Instead of 8 M KOH, 3 M KOH and 5 M KCl were used as the electrolyte in the presence of 1.4 M glycerol. The polarization curve with KCl (see Figure 3b) shows a lower performance which suggests that the glycerol fuel cell is dependent on the hydroxyl ions. Control experiments with only glycerol (1.4 M) or KOH (8 M) were also included in Figure 3a,b. No significant amount of power was generated under such conditions.
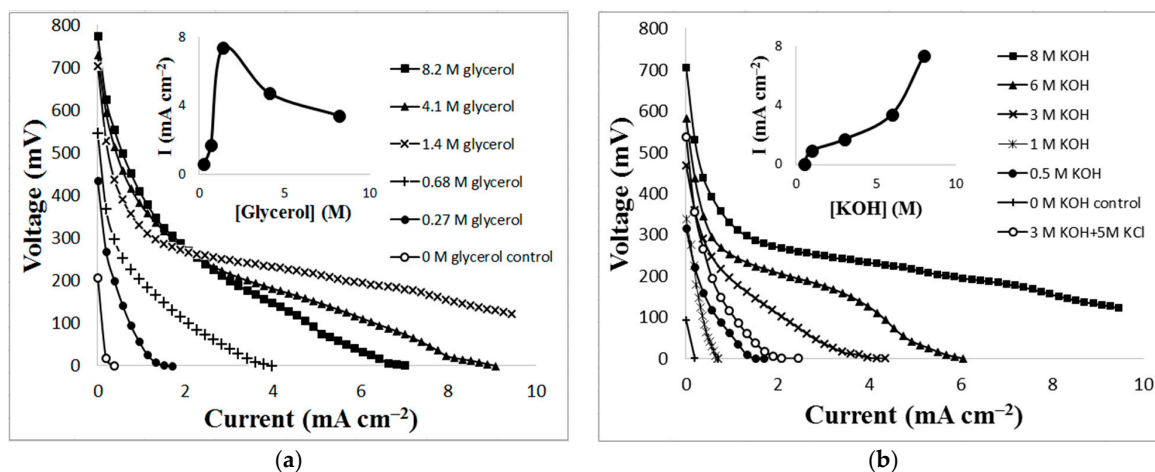

Figure 3. (**a**) Polarization curve of various concentrations of glycerol in 8 M KOH solution; (**b**) Various concentrations of KOH in 1.4 M glycerol.

Temperature effects on the power output of the glycerol fuel cell were also included in this study. Fuel cells with solutions of 8.0 M KOH and 1.4 M glycerol were placed at 4 °C, 25 °C, 35 °C, 50 °C, and 70 °C (Figure 4). The open circuit voltage increased as the temperature increased (see Table 2). However, at 25 °C, a maximum power of 1.27 mW cm^{-2} occurred at 7.39 mA cm^{-2}. As the temperatures increased to 70 °C, the maximum power decreased to 0.848 mW cm^{-2} at 2.84 mA cm^{-2}.

Table 2. The resulting open circuit voltage (mV), Maximum power (mW cm^{-2}), maximum current (mW cm^{-2}), of glycerol fuel cells in 8 M KOH and 1.4 M glycerol solutions at different temperatures.

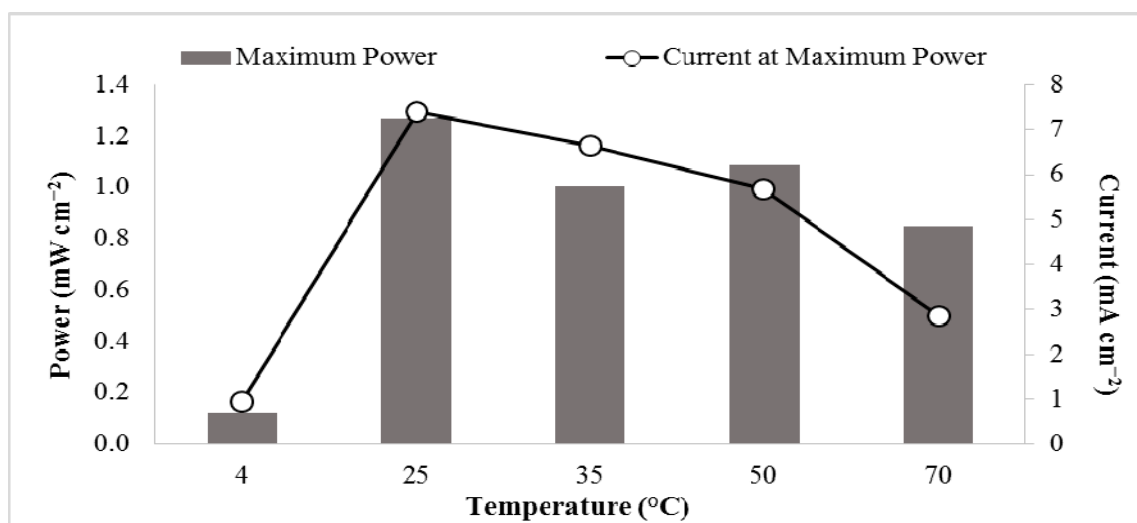| Temperature (°C)	Open Circuit Voltage (mV)	Maximum Power (mW cm^{-2})	Maximum Current (mA cm^{-2})	Voltage at Maximum Power (mV)
4	606	0.0148	0.947	130
25	704	1.27	7.39	172
35	656	1.00	6.63	152
50	696	1.09	5.68	191
70	738	0.848	2.84	375

Figure 4. Power output of 1.4 M glycerol and 8 M KOH at various temperatures, 4 °C, 25 °C, 35 °C, 50 °C and 70 °C.

To compare this cell's performance with other organic molecules that are also potential fuels, including sugars, small chain primary alcohols and other organic alcohols, this cell was also run with glucose, ethanol and xylitol as sample fuels. It was expected that these molecules would oxidize in a similar manner to the proposed oxidation of glycerol [16,17]. Each set of experiments was performed in non-optimized 8 M KOH solution with various concentrations of ethanol, xylitol, and glucose. Figure 5 displays the power production of (a) ethanol (0.218 mW cm^{-2}), (b) xylitol (0.447 mW cm^{-2}), and (c) glucose (1.74 mW cm^{-2}).
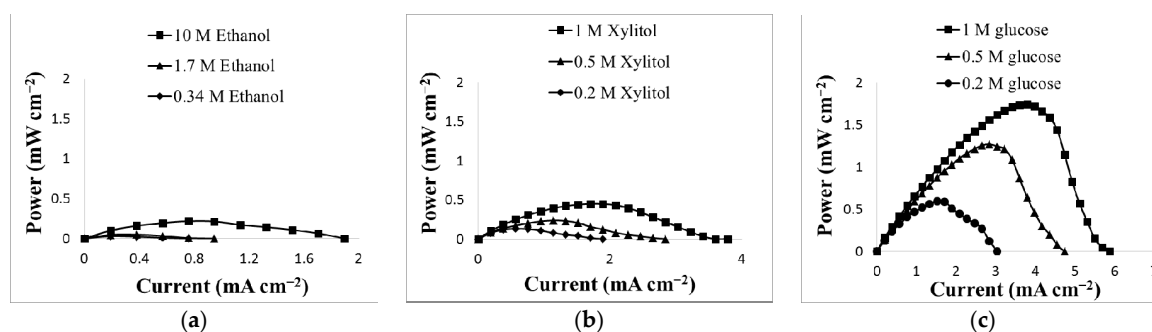

Figure 5. (**a**) Performances of various concentration of ethanol (0.34 M, 1.7 M, 10 M); (**b**) xylitol (0.2 M, 0.5 M, 1 M); (**c**) glucose (0.2 M, 0.5 M, 1 M) in 8 M KOH.

3.2. Comparison of Different Anodic Surfaces

The best performing anode surface was the gold-plated platinum mesh. Other anodic surfaces with and without gold coating in 8 M KOH and 1.4 M glycerol were also tested. Figure 6 shows the comparison of the power generated from cells using different anodic surfaces, including carbon felt and Ag-plated Ni mesh without gold-plating as controls. After gold plating these anodic surfaces, the resulting power output increased significantly. This shows the requirement for the gold atoms plated on the anodic surface, but it also indicates the impact of the different base materials of the anodic surface where the gold coating occurs. Additionally, the loss of the gold coating from carbon felt and the Ag-plated Ni surfaces was observed by the change in mass of the anodes before and after each experiment. This loss seems to be more associated with the incomplete coating process for these surfaces as opposed to any electrochemical change of the gold. There was no noticeable mass change

or observable visual loss of the gold coating on the gold-plated platinum mesh. In comparison to the gold-plated surfaces, a 99% pure gold mesh was used as an anode surface in a solution of 8 M KOH and 1.4 M glycerol. However, the performance of this gold surface was poor (see Figure 6). In fact, the performance of the gold mesh was lower than all gold-plated surfaces.
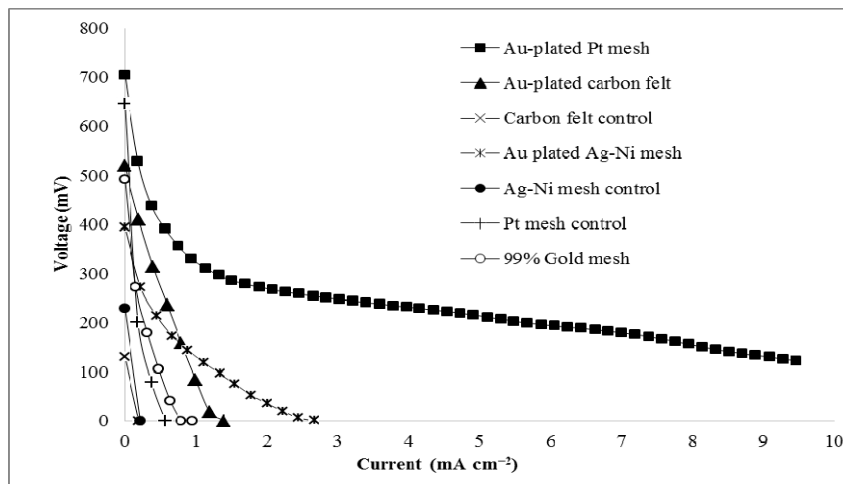

Figure 6. Polarization curves for different anodic surfaces in 8 M KOH and 1.4 M glycerol, including carbon felt with and without gold plating, Ag-plated Ni mesh with and without gold plating, platinum mesh with and without gold plating, and gold mesh.

3.3. Utilization of the Glycerol from the Transesterification of Vegetable Oil

Crude glycerol produced by transesterification of vegetable oil with methanol and KOH was also tested in the cell. The concentration of glycerol and hydroxide ion in these crude samples was determined using a standard curve that relates voltage to glycerol concentration under a constant current of 0.189 mA cm^{-2} (Figure A1a). The crude glycerol was diluted to 1.26 M and the concentration of KOH was adjusted to 8 M by measuring the pH. This allowed the comparison of optimized conditions (Figure 1a) to the crude glycerol sample. The resulting power from this experiment was 0.410 mW cm^{-2} with an open circuit voltage of 610 mV. The decrease in the power produced in this sample is likely associated with the presence of other residual chemicals from the transesterification, including left over methanol, which would compete with the glycerol in this reaction.

3.4. Mechanism Considerations

Previous work proposed that glycerol oxidation under similar conditions may result in a variety of products, including possibly H_2O_2 [16,17,24]. To identify the presence of H_2O_2, an assay utilizing the enzymatic peroxidase activity of myoglobin coupled to the color change of the electron-donating dye, ABTS, was performed (Figure A2). To ensure the activity of myoglobin was not affected by the sample, the pH of a spent fuel sample was adjusted to 7.5.

This assay did not provide evidence of the presence of hydrogen peroxide. An additional assay that utilized the increase in pressure due to the production of molecular oxygen from residual H_2O_2 was also attempted. This allowed a sample of spent fuel cell fuel to be introduced to a suspension of MnO_2. This assay also did not result in the evidence of the presence of any H_2O_2 (Figure A3a).

Proton and carbon NMR were performed on the fuel cell fuel before and after power was drawn from the cell. The comparison suggested that the glycerol in the spent fuel cell media was significantly decreased. Unfortunately, the proton NMR of the spent fuel resulted in no proton signals. This is possibly an indication of the exchanging or removal of all of the protons as in the case of a product like oxylate or metaoxylate which have been proposed as possible products for these types of oxidative surfaces [16,17,24]. ^{13}C-NMR (Figure A4) suggests that the resulting product appears to be a

carbonyl-based compound. Titrations performed did not clearly identify the pKa of the species in the sample; however, the titration curve suggests that the oxidative products are likely to be something similar to formate, carboxylate or malonate. This conclusion led to an additional use of the pressure assay to detect the production of any gas upon the acidification of the spent fuel cell sample. Upon the addition of HCl to a sample of the spent fuel in the pressure assay vessel, there was a clear release of a gas detected by an increase in the vessel's pressure (see Figure A3b). An oxygen sensor confirmed that this gas was not oxygen by showing a relative decrease in the oxygen concentration by more than 10%. The relative concentration of oxygen decreased from a relative initial amount of 98% to 86.5%. The volume that this increase in pressure occurred in was 25 mL. With the identified pressure change in this volume, it is consistent with a release on average of 1.23×10^{-4} moles of gas. This is roughly one mole of CO_2 for every mole of glycerol. This is consistent with the release of a gas other than oxygen, although the titration experiments are not clearly consistent with the presence of the carbonate ion, and there does not seem to be any major impact in terms of power decrease of the cell which might be expected upon the production of carbonates in the electrolyte.

4. Discussion

The results here clearly indicate that glycerol can be used as a fuel in these simple, membrane-less fuel cell configurations. As the concentration of glycerol increases, there is an increase in power production. The lack of linearity of power production above 2 M glycerol is interesting and worth exploring in the future. There is a possibility that as the concentration of glycerol increases, the viscosity of the solution begins to alter the activity of the glycerol at the anode surface. It is also a possibility that the higher concentration of glycerol results in the production of more carbonate product which would lower the concentration of the available activity of the electrolyte in solution. However, with 8 M KOH in solution, it is also possible that any carbonates are not significantly interfering with the required available electrolyte. The influence of the possible production of carbonates would be more pronounced over time as the cell were to run toward completion. The experiments performed where this was done to examine the products of the reaction did not show any significant decrease that would seem to be attributed to the presence of carbonates, but this is a study that should be performed in the future to identify the impact of the presence of carbonates on the cell's performance.

There is also a clear dependence on the concentration of the hydroxide ion. This concentration of hydroxide adjusts the redox potential for the glycerol and allows the reaction to occur more favorably. The fuel cell also shows a degree of activity on other small carbon alcohols including glucose, ethanol and xylitol. Besides glycerol as a fuel source, the power generated from the oxidation of glucose in this type of fuel cell setup is also relatively interesting.

According to the previous research [27], as the temperature increases, it is possible that the reaction at the cathode is limited. Secondly, based on the proposed mechanism of oxidation of glycerol [16,17], it requires oxygen to cleave the bond between Au and glycerol. The air-breathing cathode material is capable of capturing oxygen from the air. However, as the temperature increases, the solubility of oxygen decreases. Therefore, the separation between Au and glycerol oxidation product is limited. As a result, more glycerol would remain on the Au surface and would possibly interrupt the oxidation process of other glycerol molecules. Although higher temperatures might result in a faster reaction, the fact that glycerol cannot separate from the Au surface might be the main contribution to the decrease in power production.

A sample of crude glycerol from a transesterification process also produced power in this fuel cell configuration, albeit a significantly lower amount. This may be due to the concentration of glycerol being lower than what was calculated. It may be that the actual concentration of the glycerol was not attainable with the standard curve used because additional components in the solution such as methanol or soaps could interfere with the standardization of the sample. The presence of residual methanol would also compete for active sites and be oxidized itself as well. This activity would alter the current and the potential of the cell.

To produce any significant amount of power, the anodic surfaces need to have a gold-plated catalyst. Additionally, the surface under the gold plating plays a significant role. Although it is known that gold catalyzes the oxidation of glycerol [12,15–17,19], it was relatively surprising to see how poor of a catalyst gold mesh was. Based on these results, the gold surface had a lower performance compared to other gold-plated surfaces. The gold-plated platinum mesh clearly showed a much greater power generation than the gold surface. This increase in activity of the platinum anode coated in gold is likely due to the contribution that the different surfaces bring to this reaction. The platinum is possibly responsible for binding the oxygen atoms on either the glycerol molecules or possibly the needed molecular oxygen for the reaction, while the gold may kinetically favor the oxidation of the glycerol. It was also hypothesized that the different arrangement of the gold-plated atoms compared to that of the pure gold surface was responsible for the different degree of oxidation. To test this, a surface of gold mesh was gold-plated the same way the other electrodes were. The result was no improvement in the performance of the cell. This suggests that the plating method itself was not the influential part of contributing to the improved oxidation of glycerol. This is a clear indication that the best catalyst for glycerol oxidation is likely going to require at least two different elements.

By performing various assays, it is clear that there was no detectable H_2O_2 produced from the oxidation that occurs in this cell. It is possible that the cathode material which contains MnO_2 promotes the decomposition of H_2O_2. Thus it could be conceived that H_2O_2 produced from the oxidation of glycerol would be immediately decomposed into O_2 and H_2O at the cathode. This is unlikely to occur so quickly and it would still seem possible to identify some residual peroxide if it was being produced at the anode and needing to migrate to the cathode to be consumed. This process would also seem to be associated with a decrease in voltage of the individual runs as this theoretical concentration of H_2O_2 is accumulated. Such a shift in voltage is not seen within the individual runs.

It was interesting to see that after acidifying the spent fuel sample, a distinct pressure increase was detected. Identifying the gas produced upon acidifying the spent fuel sample will help clarify the products from this glycerol oxidation, but with the concentration of oxygen decreasing upon the production of this gas, it is clearly not oxygen. The pressure results are consistent with the presence of the carboxylate ion. Therefore, it is a possibility that the oxidation of glycerol in this fuel cell results in a decarboxylation which releases CO_2. Assuming that the gas generated was CO_2, the CO_2 generated from decarboxylation should have a ratio of 1:1 with glycerol as it is less likely that the resulting two carbon species would be able to further decompose to another unit of carboxylate. The resulting calculations of the volume of gas produced is very close this ratio.

Additionally, this cell configuration was able to endure over 150 runs without any indication of power decrease due to the possible accumulation from the product on the cathodic or anodic surfaces. According to the mechanism proposed [16,17], molecules leave the surfaces after being reacted which would be consistent with the longevity of these cells. As a result, it is likely that the accumulations from the products of this oxidation process are minimal which result in no indication of power decrease.

To further investigate the product of the glycerol oxidation, experiments which were run so that the fuel in the fuel cell was completely oxidized were used to count the amount of electrons that transferred from the glycerol. According to the resulting calculations, these experiments are very close to the electrons transferable from glycerol, assuming an oxidation to CO_2. This is further evidence to suggest that the glycerol is significantly oxidized.

5. Conclusions

This simple cell design was easy to organize, easy to operate, and was able to promote the oxidation of glycerol and generate power. Through examining different concentrations of electrolyte and fuel sources on different anodic surfaces, it was possible to demonstrate the effects from such combinations and various anodic surfaces. The most impressive combination was the MnO_2 cathode with the gold-plated platinum mesh with 1.4 M glycerol and 8.0 M KOH. Additionally, it has been demonstrated that there is a feasibility of using crude glycerol as a fuel source with this fuel cell

configuration to generate power. The cell performance could likely be further optimized for the crude glycerol samples, which include additional byproducts from the transesterification, by adjusting KOH and crude glycerol concentrations. The performance of a peroxidase assay and pressure assays confirmed that there was no detectable H_2O_2 in the spent fuel sample but that there is likely the carboxylate ion which is not inconsistent with ^{13}C-NMR (Figure A4). Further determination of the final products of the glycerol oxidation is another interesting area which could be further researched.

Author Contributions: Conceptualization, D.S.; Methodology, D.S.; Validation, D.S.; Formal Analysis, D.S.; Investigation, Y.J.T.; Resources, D.S.; Data Curation, Y.J.T.; Writing-Original Draft Preparation, Y.J.T.; Writing-Review & Editing, D.S.; Visualization, D.S. and Y.J.T.; Supervision, D.S.; Project Administration, D.S. and Y.J.T.; Funding Acquisition, D.S.

Conflicts of Interest: The authors declare no conflict of interest.

Appendix

Table A1. A list of references which used membranes as an important component of the fuel cells.

Cathode	Anode	Membrane	Reported Max Power	Open Circuit Voltage	Reference Number
Air breath cathode material (See Section 2.2)	With and without Au-plated Pt mesh, Ag-plated Ni mesh, carbon felt	N/A	1.27 mW cm^{-2}	704 mV	Current research
Pt/C loaded on ELAT Gas Diffusion Layer	Pt/C loaded carbon cloth	Polybenzimidazole membrane	≈24 mW cm^{-2}	≈720 mV	10
Pt wire	NiPi/Pi-Fe$_2$O$_3$ film	Nafion membrane	0.11 mW cm^{-2}	480 mV	11
Pt/C loaded on ELAT Gas Diffusion Layer	Pt/C loaded carbon cloth	Polybenzimidazole membrane	35 mW cm^{-2}	≈800 mV	14
Ionomer coated anion exchange membrane	Pd-based anode catalysts	Anion exchange membrane DAFCs	276.2 mW cm^{-2}	≈975 mV	18
Pt/C loaded metal	Pd/C or PdAu/C loaded metal	Fumasep-FAA-PEEK membrane	34 mW cm^{-2}	720 mV	19
ELAT electrode with 20% Pt	Oxalate oxidase on E-TEK TGP060 Toray paper	TBAB-modified Nafion membrane	1.32 mW cm^{-2}	value not reported	20
Pt black on carbon gas diffusion layer	Palladium black on carbon cloth	Anion exchange membrane	78 mW cm^{-2}	≈325 mV	21
Fe-Cu-based cathode	Au/C catalyzed dissusion layer	Anion-exchange membrane	43.9 mW cm^{-2}	≈900 mV	22
20 wt% Pd/C on carbon	Pd, PdAu, PdSn or PdAuSn on carbon	Fumasep-FAA3-PEEK membrane	51 mW cm^{-2}	≈900 mV	23
Acta 4020 catalyzed cathode	Pd/CNT, PdAg/CNT, and Ag/CNT catalyst on carbon cloth	Anion-exchange membrane	≈75 mW cm^{-2}	≈830 mV	24

(a)　　　　　　　　　　　　(b)

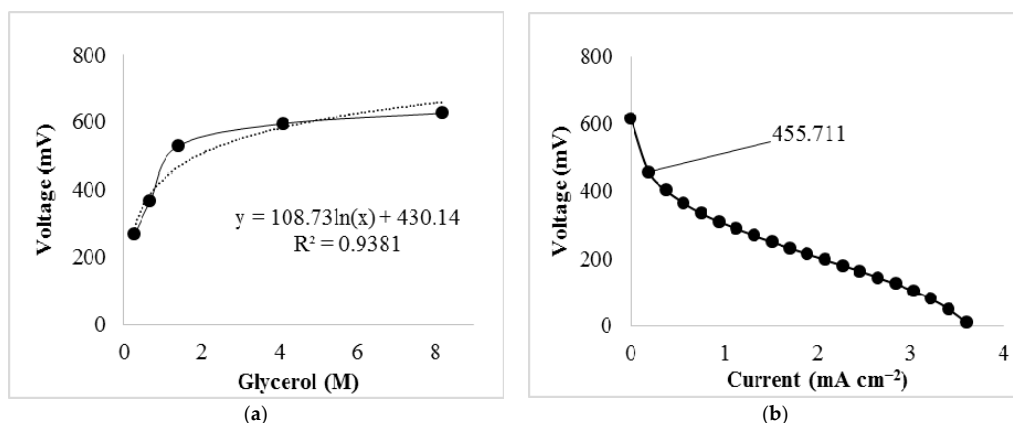**Figure A1.** (**a**) Standard curve created by plotting the voltage change of varying concentrations of glycerol in 8 M KOH at 1 mA; (**b**) Polarization curve of a diluted crude glycerol sample from which the labeled voltage was used to determine the concentration of crude glycerol according to the equation expressed in (**a**).
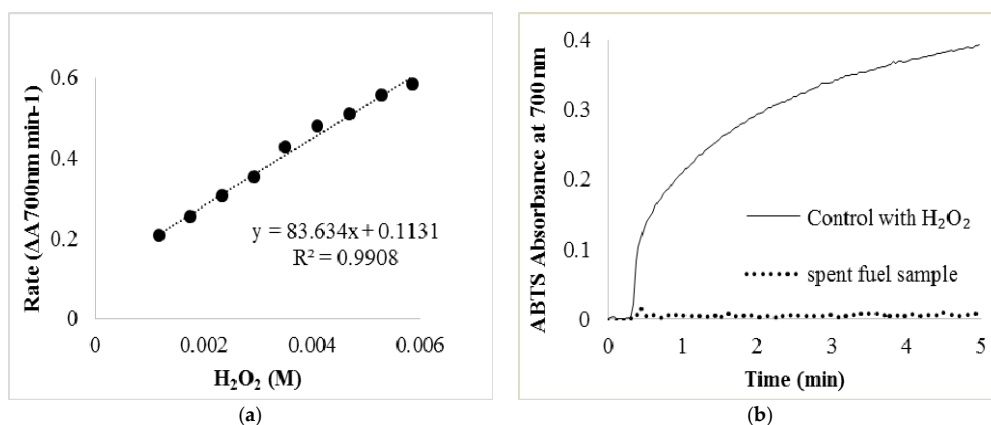

(a)　　　　　　　　　　　　(b)

Figure A2. (**a**) ABTS assay standard curve based on the enzyme activities of myoglobin which was used to identify the concentration of H_2O_2 in the solution after glycerol oxidation; (**b**) One of the curves with 0.02 mL H_2O_2 comparing with spent fuel sample from glycerol oxidation. The control is 0.02 mL of H_2O_2 in 0.2 mL ABTS, 2.6 mL of pH 7.5 Tris buffer, and 0.2 mL of 1 mg mL^{-1} myoglobin. In spent fuel sample, no H_2O_2 was added additionally.
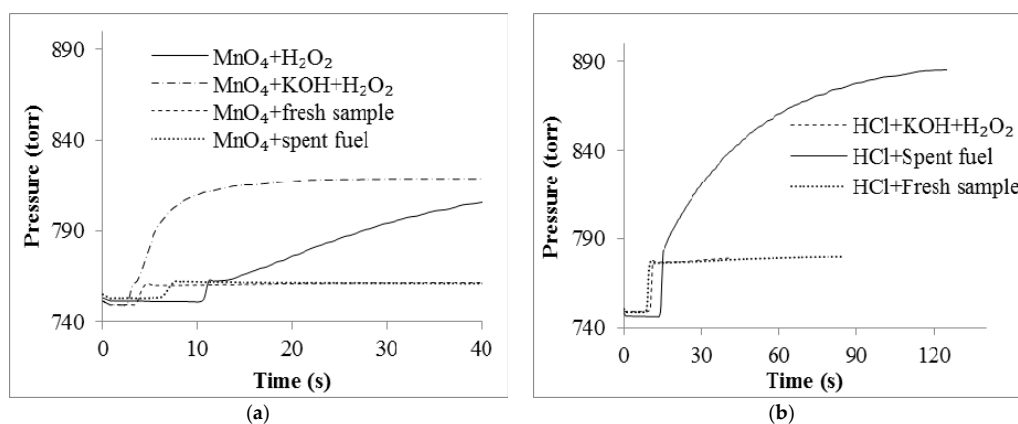

(a)　　　　　　　　　　　　(b)

Figure A3. (**a**) Pressure assay with suspension of MnO_2. Control 1 is suspension of MnO_2 with 100 μL H_2O_2. Control 2 is suspension of MnO_2 with 100 μL H_2O_2 in 8M KOH; (**b**) Acidify pressure assay curve where the control is 1M HCl 8M KOH + 100 μL H_2O_2. The initial rate in terms of pressure and time was determined through the slope of the trend line.
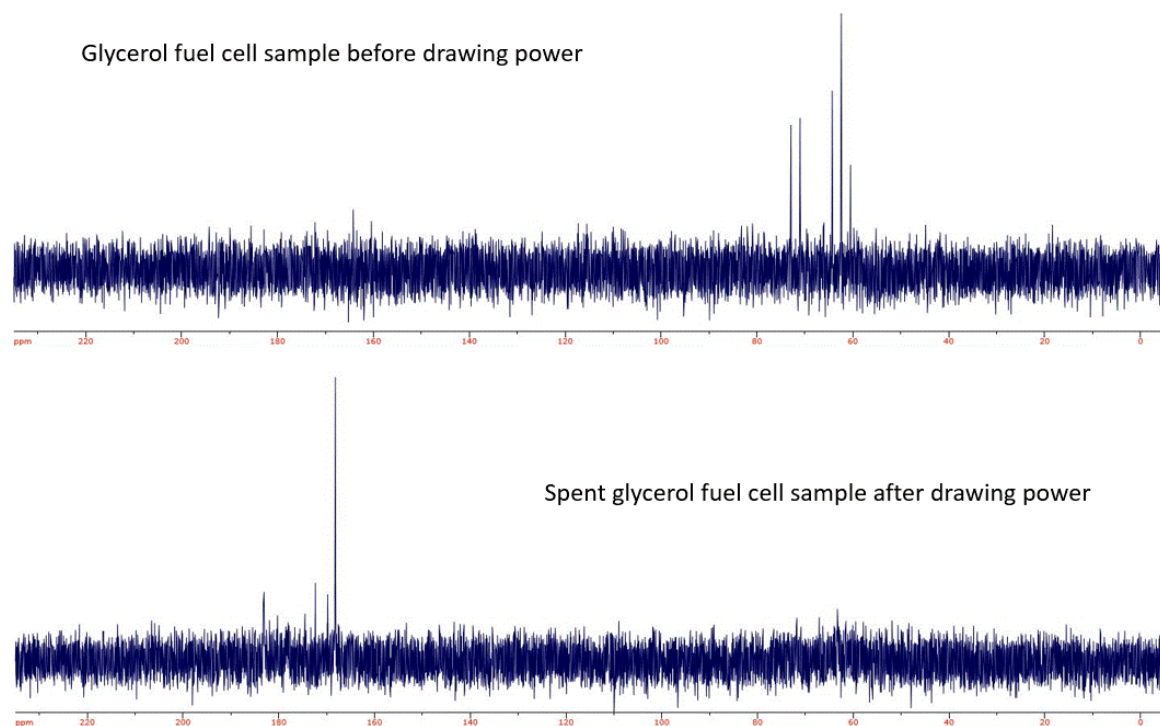
Figure A4. ^{13}C-NMR of a glycerol fuel cell solution before (**above**) and after (**below**) drawing power from the fuel cell. After the fuel cell solution is spent the signal for the glycerol falls into the noise and the emerging signals are consistent with carbonyl carbons.

References

1. Sawin, J.L.; Moomaw, W.R. *Renewable Revolution: Low-Carbon Energy by 2030*; Worldwatch Insititute: Washington, DC, USA, 2009; pp. 1–51.
2. Zhang, N.; Lior, N.; Jin, H. The energy situation and its sustainable development strategy in China. *Energy* **2011**, *36*, 3639–3649. [CrossRef]
3. Araújo, K.; Mahajan, D.; Kerr, R.; Silva, M. Global biofuels at the crossroads: An overview of technical, policy, and investment complexities in the sustainability of biofuel development. *Agriculture* **2017**, *7*, 32. [CrossRef]
4. Binhayeeding, N.; Klomklao, S.; Sangkharak, K. Utilization of waste glycerol from biodiesel process as a substrate for mono-, di-, and triacylglycerol production. *Energy Procedia* **2017**, *138*, 895–900. [CrossRef]
5. Lin, Y. Catalytic valorization of glycerol to hydrogen and syngas. *Int. J. Hydrogen Energy* **2013**, *38*, 2678–2700. [CrossRef]
6. Haider, M.H.; Dummer, N.F.; Knight, D.W.; Jenkins, R.L.; Howard, M.; Moulijn, J.; Taylor, S.H.; Hutchings, G.J. Efficient green methanol synthesis from glycerol. *Nat. Chem.* **2015**, *7*, 1028–1032. [CrossRef] [PubMed]
7. Speers, A.M.; Young, J.M.; Reguera, G. Fermentation of glycerol into ethanol in a microbial electrolysis cell driven by a customized consortium. *Environ. Sci. Technol.* **2014**, *48*, 6350–6358. [CrossRef] [PubMed]
8. Bohon, M.D.; Metzger, B.A.; Linak, W.P.; King, C.J.; Roberts, W.L. Glycerol combustion and emissions. *Proc. Combust. Inst.* **2011**, *33*, 2717–2724. [CrossRef]
9. Arechederr, R.L.; Treu, B.L.; Minteer, S.D. Development of glycerol/O$_2$ biofuel cell. *J. Power Sources* **2007**, *173*, 156–161. [CrossRef]
10. Nascimento, A.P.; Linares, J.J. Performance of a direct glycerol fuel cell using KOH doped polybenzimidazole as electrolyte. *J. Braz. Chem. Soc.* **2014**, *25*, 509–516. [CrossRef]
11. Chong, R.; Wang, B.; Li, D.; Chang, Z.; Zhang, L. Enhanced photoelectrochemical activity of Nickel-phosphate decorated phosphate-Fe$_2$O$_3$ photoanode for glycerol-based fuel cell. *Sol. Energy Mater. Sol. Cells* **2017**, *160*, 287–293. [CrossRef]

12.	Yahya, N.; Kamarudin, S.K.; Karim, N.A.; Masdar, M.S.; Loh, K.S. Enhanced performance of a novel anodic PdAu/VGCNF catalyst for electro-oxidation in a glycerol fuel cell. *Nanoscale Res. Lett.* **2017**, *12*. [CrossRef] [PubMed]

13.	Li, N.; Xia, W.; Xu, C.; Chen, S. Pt/C and Pd/C catalysts promoted by Au for glycerol and CO electrooxidation in alkaline medium. *J. Energy Inst.* **2005**, *90*, 725–733. [CrossRef]

14.	Frota, E.F., Jr.; de Barros, V.V.S.; de Araújo, B.R.S.; Purgatto, A.G.; Linares, J.L. Pt/C containing different platinum loadings for use as electrocatalysts in alkaline PBI-based direct glycerol fuel cells. *Int. J. Hydrogen Energy* **2017**, *42*, 23095–23106. [CrossRef]

15.	Pulido, D.F.Q.; Kortenaar, M.V.T.; Hurink, J.L.; Smit, G.J.M. A practical approach in glycerol oxidation for the development of a glycerol fuel cell. *Trends Green Chem.* **2017**, *3*. [CrossRef]

16.	Villa, A.; Dimitratos, N.; Chan-Thaw, C.E.; Hammond, C.; Prati, L.; Hutchings, G.J. Glycerol Oxidation Using Gold-Containing Catalysts. *Acc. Chem. Res.* **2015**, *48*, 1403–1412. [CrossRef] [PubMed]

17.	Wang, D.; Villa, A.; Su, D.S.; Prati, L.; Schlögl, R. Carbon-supported gold nanocatalysts: shape effect in the selective glycerol oxidation. *ChemCatChem* **2013**, *5*, 2717–2723. [CrossRef]

18.	Qi, J.; Benipal, N.; Liang, C.; Li, W. PdAg/CNT catalyzed alcohol oxidation reaction for high-performance anion exchange membrane direct alcohol fuel cell (alcohol = methanol, ethanol, ethylene glycol and glycerol). *Appl. Catal. B Environ.* **2016**, *199*, 494–503. [CrossRef]

19.	Geraldes, A.N.; Silva, D.F.; Silva, J.C.M.; Souza, R.F.B.; Spinacé, E.V.; Neto, A.O.; Linardi, M.; Santos, M.C. Glycerol electrooxidation in alkaline medium using Pd/C, Au/C and PdAu/C electrocatalysts prepared by electron beam irradiation. *J. Braz. Chem. Soc.* **2014**, *25*, 831–840. [CrossRef]

20.	Arechederra, R.L.; Minteer, S.D. Complete oxidation of glycerol in an enzymatic biofuel cell. *Fuel Cells* **2008**, *9*, 63–69. [CrossRef]

21.	Tran, K.; Nguyen, T.Q.; Bartrom, A.M.; Sadiki, A.; Haan, J.L. A fuel-flexible alkaline direct liquid fuel cell. *Fuel Cells* **2014**, *14*, 834–841. [CrossRef]

22.	Han, X.; Chadderdon, D.J.; Qi, J.; Xin, L.; Li, W.; Zhou, W. Numerical analysis of anion-exchange membrane direct glycerol fuel cells under steady state and dynamic operations. *Int. J. Hydrogen Energy* **2014**, *39*, 19767–19779. [CrossRef]

23.	Geraldes, A.N.; Silva, D.F.; da Silva, L.G.; Spinacé, E.V.; Neto, A.O.; Santos, M.C. Binary and ternary palladium based electrocatalysts for alkaline direct glycerol fuel cell. *J. Power Sources* **2015**, *293*, 823–830. [CrossRef]

24.	Benipal, N.; Qi, J.; Liu, Q.; Li, W. Carbon nanotube supported PdAg nanoparticles for electrocatalytic oxidation of glycerol in anion exchange membrane fuel cells. *Appl. Catal. B Environ.* **2017**, *210*, 121–130. [CrossRef]

25.	Garland, N.L.; Papageorgopoulos, D.C.; Stanford, J.M. Hydrogen and fuel cell technology: Progress, challenges, and future directions. *Energy Procedia* **2012**, *28*, 2–11. [CrossRef]

26.	Inoue, A.; Shimizu, T.; Yamaura, S.; Fujita, Y.; Takagi, S.; Kimura, H. Development of glassy alloy separators for a proton exchange membrane fuel cell (PEMFC). *Mater. Trans.* **2005**, *46*, 1706–1710. [CrossRef]

27.	Orton, D.; Scott, D. Temperature dependence of an abiotic glucose/air alkaline fuel cell. *J. Power Sources* **2015**, *295*, 92–98. [CrossRef]